Biochemistry

 Volume 36, Number 7 February 18, 1997

Accelerated Publications

The Structure of the Superantigen Exfoliative Toxin A Suggests a Novel Regulation as a Serine Protease[†,‡]

Gregory M. Vath,[§] Cathleen A. Earhart,[§] James V. Rago,[∥] Michael H. Kim,[∥] Gregory A. Bohach,[⊥] Patrick M. Schlievert,[∥] and Douglas H. Ohlendorf*[,§]

Departments of Biochemistry and Microbiology, University of Minnesota Medical School, Minneapolis, Minnesota 55455, and Department of Microbiology, Molecular Biology, and Biochemistry, University of Idaho, Moscow, Idaho 83843

Received October 17, 1996; Revised Manuscript Received December 17, 1996[⊗]

ABSTRACT: Exfoliative toxin A (ETA) causes staphylococcal scalded skin syndrome which is characterized by a specific intraepidermal separation of layers of the skin. The mechanism by which ETA causes skin separation is unknown although protease or superantigen activity has been implicated. The X-ray crystal structure of ETA has been solved in two crystal forms to 2.1 and 2.3 Å resolution and *R*-factors of 17% and 19%, respectively. The structures indicate that ETA belongs to the chymotrypsin-like family of serine proteases and cleaves substrates after acidic residues. The conformation of a loop adjacent to the catalytic site is suggested to be key in regulating the proteolytic activity of ETA through controlling whether the main chain carbonyl group of Pro192 occupies the oxyanion hole. A unique amino-terminal domain containing a 15-residue amphipathic α helix may also be involved in protease activation through binding a specific receptor. Substitution of the active site serine residue with cysteine abolishes the ability of ETA to produce the characteristic separation of epidermal layers but not its ability to induce T cell proliferation.

Staphylococcal exfoliative (or epidermolytic) toxins (ETs), designated serotypes A and B (ETA and ETB),[1] are made by approximately 5% of *Staphylococcus aureus* strains and are the causative agents in staphylococcal scalded skin syndrome (Melish et al., 1972). This illness is primarily seen in newborns and is characterized by specific intraepidermal separation of the layers of skin between the stratum spinosum and the stratum granulosum. The illness begins abruptly with a generalized erythema, usually around the mouth, and spreads over the entire body. When the skin is gently rubbed the epidermis irreversibly wrinkles, giving rise to the characteristic Nikolsky sign. Complete separation of the epidermis at the desmosomes follows with the appearance of large sterile blisters. Although the cause of the epidermal separation has remained elusive, investigators have hypothesized at least three mechanisms: protease activity (Wuepper et al., 1975), ability to induce edema (Rogolsky, 1979), and superantigenic activity (Marrack & Kappler, 1990).

The genes *eta* and *etb* have been cloned and their amino acid sequences deduced (Lee et al., 1987; O'Toole & Foster,

[†] Supported by NIH Grants HL-36611, GM-54384, and AI-28401.

[‡] The coordinates of exfoliative toxin A have been deposited in the Protein Data Bank (entry number 1EXF for the tetragonal form; entry number 2EXF for the monoclinic form).

[§] Department of Biochemistry, University of Minnesota Medical School.

[∥] Department of Microbiology, University of Minnesota Medical School.

[⊥] University of Idaho.

[⊗] Abstract published in *Advance ACS Abstracts,* February 1, 1997.

[1] Abbreviations: ETA, exfoliative toxin A; ETB, exfoliative toxin B; DFP, diisopropyl phosphofluoridate; PMSF, phenylmethanesulfonyl fluoride; TSST-1, toxic shock syndrome toxin 1; SE, staphylococcal enterotoxin; PEG, poly(ethylene glycol); PBS, phosphate-buffered saline; RMS, root-mean-square; Glu-SGP, glutamic acid specific *Streptomyces griseus* protease; SGP-A, *S. griseus* protease A; SGP-B, *S. griseus* protease B.

S0006-2960(96)02614-1 CCC: $14.00

1987). The mature proteins of ETA and ETB are 242 and 246 residues, respectively, after their signal sequences are cleaved. The ETs are about 40% identical with each other with no apparent sequence homology to other bacterial toxins. The ETs have been found to be about 25% identical with staphylococcal V8 protease (Dancer et al., 1990; Bailey & Smith, 1990).

Several studies have suggested the ETs function as serine proteases though peptide bond cleavage has not been reported [for a review see Bailey et al. (1995)]. Early studies were unable to demonstrate inhibition of skin separation in vivo or in vitro by various protease inhibitors (McLay et al., 1975; Elias et al., 1977; Nishioka et al., 1981). Later Dancer et al. (1990) reported the serine protease inhibitors DFP and PMSF increased the time needed for ETA to show skin separation of newborn mice in vivo. Bailey and Smith (1990) predicted that Ser195 of ETA is the catalytic residue, similar to the active site Ser195 of chymotrypsin, by radiolabeling with the [^{3}H]DFP which covalently modifies the catalytic serine residue in serine proteases even though only 6% of the ETA sample was labeled. Other reports have demonstrated that single site mutations of the Ser, His, or Asp residues proposed to be part of the catalytic triad of ETA abolished skin separation activity (Redpath et al., 1991; Prevost et al., 1991, 1992).

Other studies have suggested that the ETs belong to the family of proteins referred to as superantigens [for a review see Marrack and Kappler (1990)]. Initial reports of Morlock et al. (1980) demonstrated that ETA is mitogenic for murine T lymphocytes. Later Marrack and Kappler (1990) indicated that ETA is a superantigen which stimulates the expansion of human Vβ2$^+$ T lymphocytes as does toxic shock syndrome toxin 1 (TSST-1). Superantigens with known tertiary structures include TSST-1 (Prasad et al., 1993; Acharya et al., 1994) and the staphylococcal enterotoxins (SE) SEA (Schad et al., 1995), SEB (Swaminathan et al., 1992), SEC2 (Papageorgiou et al., 1995), and SEC3 (Hoffmann et al., 1994).

We report the structure of two crystal forms of ETA to high resolution and suggest that skin separation is caused by proteolytic activity independent of mitogenicity.

METHODS

Protein Purification. Exfoliative toxin A was purified from *S. aureus* strain MN EV (Lee et al., 1991) as well as from *S. aureus* RN4220 containing pCE104 (a shuttle vector consisting of the staphylococcal plasmid pE194 and pUC18) in which the wild-type and mutant S195C *eta* gene had been inserted (Murray et al., 1995). For the S195C mutant the entire gene was sequenced to ensure that the only change occurred at position 195.

Bacteria were grown at 37 °C with aeration in a dialyzed beef heart medium, either with or without the addition of 2% tryptone, until stationary phase (Bohach et al., 1990). Cultures of RN4220 containing the mutant *eta* included 5 μg/mL erythromycin. Upon harvesting, the cultures were treated with 4 volumes of absolute ethanol for 2 days. The precipitates were collected, suspended in distilled water, centrifuged to remove insoluble material (10000*g*, 30 min), and dialyzed for 24 h at 4 °C against water. The dialyzate was subjected to thin-layer isoelectric focusing first in a pH 3.5−10 gradient and then in a pH 6−8 gradient. The purified toxins were dialyzed 4 days against distilled water to remove ampholytes. Typically 2 mg of ETA was obtained per liter of culture fluid.

Table 1: Data Collection, SIRAS, and Refinement Statistics

	native I	native II	native III	native IV	ammonium diuranate
diffraction data					
space group	$P2_1$	$P2_1$	$P2_1$	$P4_32_12$	$P4_32_12$
cell dimensions					
a (Å)	49.6	48.8	49.7	71.5	
b (Å)	67.4	67.4	67.7	71.5	
c (Å)	82.6	45.2	81.5	122.86	
β (deg)	93.4	114.5	90.4		
mol/ASU	2	1	2	1	1
resolution (Å)	26−2.1	25−2.3	15−2.5	17−2.1	17−2.8
redundancy	3.5	4.3	4.0	4.5	4.0
completeness (%)	87.0	98.0	92.0	92.0	90.0
R-merge (%)[a]	5.55	6.45	7.15	7.23	8.40
SIRAS					
$\Delta F/F$ (%)[b]					10.2
CullR_centric[c]					0.67
phasing power[d]					1.21
figure of merit					0.39
refinement					
reflections		10963		16869	
R-factor (%)		18.9		17.2	
R_{free} (%)		26.7		20.5	
RMS bond length (Å)		0.006		0.006	
RMS bond angle (deg)		1.7		1.5	
average *B*-factor (Å^2)		29.4		22.2	

[a] $R\text{-merge} = \sum_{hkl}\sum_i|I_i(hkl)_i - \langle I(hkl)\rangle|/\sum_{hkl}\sum_i I_i(hkl)$. [b] $\Delta F/F = \sum|F_P - F_{PH}|/\sum F_P$. [c] $\text{CullR\_centric} = \sum_{hkl}||F_{PH} \pm F_P| - F_{H(calc)}|/\sum_{hkl}|F_{PH} - F_H|$. [d] $\text{Phasing power} = \sum_{hkl}F_H/\sum_{hkl}|F_{PH(obs)} - F_{PH(calc)}|$.

Structure Determination. Crystals of wild-type ETA were obtained by vapor diffusion using the hanging drop method. Purified ETA protein was concentrated to 10 mg/mL using a Centricon-3 microconcentrator (Amicon, Beverly, MA). Two microliters of this solution was mixed with 2 μL of 100 mM cacodylate buffer, pH 6.5, 29% PEG 8000, and 200 mM ammonium sulfate on a siliconized coverslip. The coverslip was then inverted over a well containing 1 mL of the mother liquor and incubated at 4 °C. These conditions produced crystal forms I, II, and III although no drop had more than one crystal form. Crystal form IV was similarly obtained with the inclusion of 10% 2-propanol. Crystal form I had been reported earlier under slightly different conditions (Yoo et al., 1978). Form II crystals were small, requiring macroseeding. Diffraction data were collected on a Siemens area detector using monochromated Cu Kα radiation produced by a Rigaku RU-200B rotating anode and processed using the XENGEN software package (Howard et al., 1987). Data collection statistics for the four crystal forms of ETA are presented in Table 1.

Soaking form IV crystals of ETA for 3 weeks at 4 °C in mother liquor saturated with ammonium diuranate produced a single site derivative that could be solved by Patterson methods. Single isomorphous replacement with anomalous signal (SIRAS) phases were calculated using MLPHARE and the CCP4 program suite (Collaborative Computational Project, 1994). Solvent flattening with the DM program (Cowtan, 1994) (60% solvent content and automated skeletonization) produced an interpretable electron density map.

The initial ETA model was built in a 2.8 Å resolution electron density map with the program MAID (Levitt & Banaszak, 1993). Refinement of the initial model using the

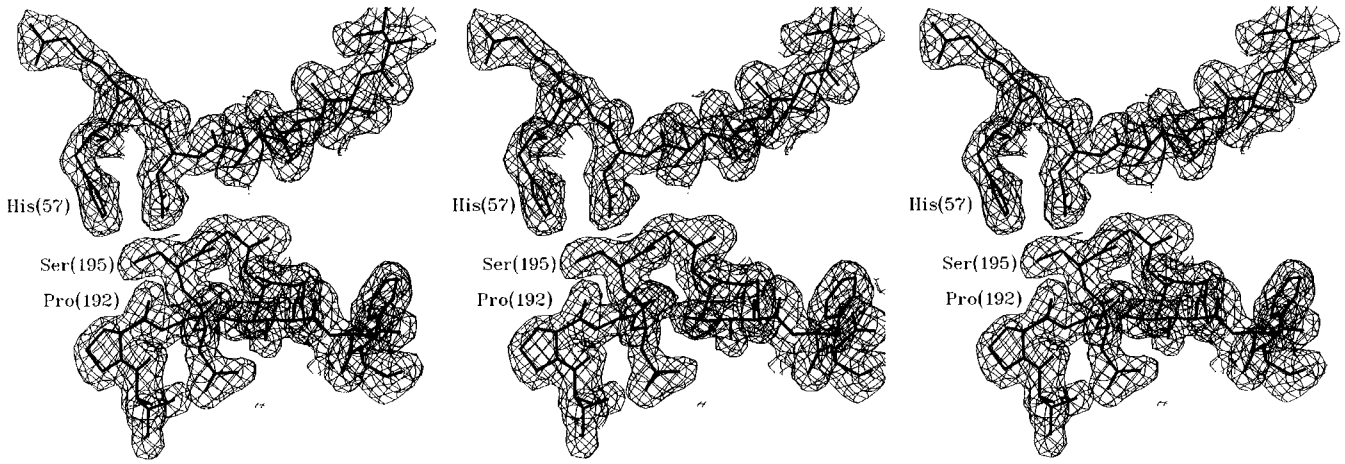

FIGURE 1: $2F_o - F_c$ electron density map calculated after a cycle of refinement in which His(57), Asp(102), Pro(192), Gly(193), and Ser(195) were omitted. The map is contoured at 1.0σ with the final model of crystal form IV included. In this and subsequent stereo drawings residues are numbered on the basis of chymotrypsin numbering, and the left pair of figures gives a "wall-eye" stereo while the right pair gives a "cross-eye" stereo.

simulated annealing protocol in X-PLOR (Brünger, 1990) with data between 5 and 2.8 Å and $F > 2\sigma$ resulted in an *R*-factor of 25% and an R_{free} (10% removed) of 34%. Subsequent model building including positional and *B*-factor refinement using all data ($F > 0$) between 17 and 2.1 Å and a bulk solvent correction brought the *R*-factor to 18% and the R_{free} to 23%. Water molecules were added with the following criteria: $F_o - F_c$ density $>4\sigma$, $2F_o - F_c$ density $>1\sigma$, and within 3.4 Å of a hydrogen bond donor or acceptor. A $+8\sigma$ feature in the $F_o - F_c$ map was interpreted in the last stages of refinement as a free glycine (Gly300) due to the shape of the feature and its surrounding environment, i.e., residues Lys32(21),[2] Arg38(26A), and Asn91(71). The feature was not consistent with any component in the crystallization solutions, e.g., cacodylate. There have been no reports of glycine associating with or affecting the activity of ETA. The final refined model of ETA in crystal form IV includes 241 residues, 107 water atoms, and a free glycine. The *R*-factor including all data ($F > 0$) from 17 to 2.1 Å with a bulk solvent correction is 17.2% and the R_{free} is 20.5%. Representative electron density for the refined model is shown in Figure 1.

The positions of the molecule(s) in crystal forms I, II, and III were determined using AMORE (Navaza, 1994) and the molecular replacement package in CCP4 with a partially refined model from crystal form IV. The rotation and translation solutions were unambiguous. Rigid body refinement in X-PLOR produced *R*-factors for the models of crystal forms I, II, and III of 43%, 37%, and 34%, respectively. Simulated annealing was used as for crystal form IV. Forms I and III failed to refine properly as indicated by increases in their respective R_{free}'s while their *R*-factors fell. The model for crystal form II refined well giving an *R*-factor of 18% and an R_{free} of 27%. Subsequent refinement of the model for crystal form II proceeded as with that for crystal form IV including the addition of a free glycine. The final model for crystal form II includes 241 residues, 40 water molecules, and a free glycine. Using all data between 25 and 2.3 Å resolution the final model with a bulk solvent correction has an *R*-factor of 18.9% and an R_{free} of 26.7%. Table 1 summarizes the data collection, SIRAS, and refinement statistics for the various crystal forms of ETA.

Visualization of the molecules and least squares superposition were done using O (Jones et al., 1991). Geometric parameters of the models were checked using PROCHECK (Laskowski et al., 1993).

Biological Assays. The capacity of recombinant wild-type and S195C ETA to induce proliferation of human T lymphocytes was evaluated in quadruplicate by measuring the incorporation of [^{3}H]thymidine into DNA over a 4 day period (Barsumian et al., 1978). The ability of ETA to cause the separation of layers of the skin was evaluated in 2−3 day old BALB/c mice (National Cancer Institute, Fredericksburg, MD) (Melish & Glasgow, 1972). Ten micrograms of wild-type and mutant ETA was injected with phosphate-buffered saline (PBS) (0.005 M sodium phosphate, pH 7.2, 0.15 M NaCl) intracutaneously in the nape of the neck in 50 μL volumes (3 mice/group). Control mice received 50 μL of PBS. Three mice per group also received 10 μg of either trypsin type III (Sigma Chemical Co., St. Louis, MO) or subtilisin (Sigma). Animals were examined for positive Nikolsky signs (irreversible wrinkling) hourly by gentle stroking of the neck.

RESULTS AND DISCUSSION

The final model of ETA in crystal form IV has 91% of the residues in the most favorable Ramachandran regions with only one residue [Leu217(220)] in a disallowed region. The amino-terminal residue was not visible in the $2F_o - F_c$ map and was not included in the model. Also, the side chains of Glu5(1E), Glu6(1F), Lys36(25), and Arg219(221A) had no $2F_o - F_c$ density beyond Cβ and were modeled as alanines. ETA in crystal form II has 90% of the residues in the most favorable region with Leu217(220) again being the only outlier. The amino terminal residue was also not visible in the $2F_o - F_c$ map and not included in the final refined model. The four side chains mentioned above were, however, visible in the $2F_o - F_c$ map of ETA form II. The conformations of these side chains were included in the final ETA model of crystal form IV with zero occupancy.

Two crystal forms of ETA (I and III) failed to refine properly. Calculation of the Pattersons using data from 10

[2] Primary sequence numbers refer to the linear sequence of the mature protein except where noted. The residue numbers enclosed in parentheses refer to topological equivalences of α-chymotrypsinogen [see Bode et al. (1989)].

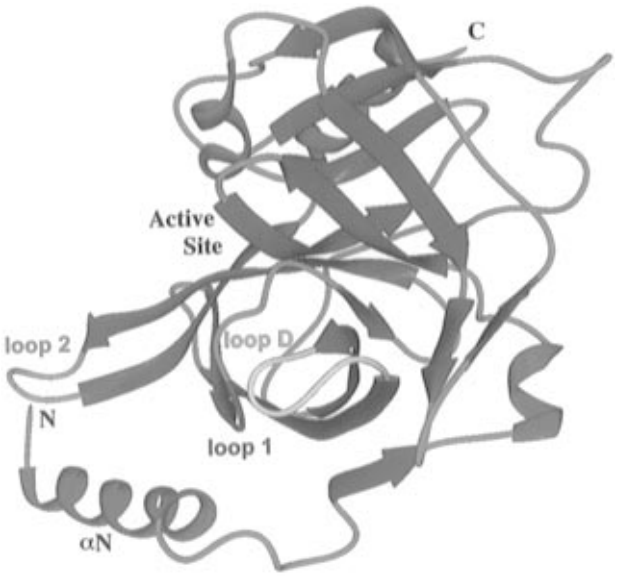

FIGURE 2: Ribbon diagram of the structural elements of ETA. Helices are in red; β strands are in blue; loops 1, 2, and D are in magenta, cyan, and yellow, respectively. This figure defines the standard orientation used in the other figures.

to 4 Å resolution for these crystal forms had extremely strong features (~30% of the origin peak) at ($u = 0.6$, $v = 0.0$, $w = 0.5$) and ($u = 0.5$, $v = 0.0$, $w = 0.5$), respectively. For crystal form III, the peak was consistent with pseudo-B-centering. Exact B-centering reduces the unit cell of crystal form III to the primitive unit cell of crystal form II. In crystal form I the Patterson feature indicates that the identically oriented molecules are ~5 Å closer together than in crystal form III. Thus small shifts in half the molecules in the crystals produced the three observed crystal forms. This relation suggests that some form of translational twinning may be responsible for the inability to obtain accurate models for crystal forms I and III.

The only agents shown to inhibit the skin separation activity of ETA in vivo or in vitro have been chelating agents. Because of these results it has been proposed that ETA binds a metal cofactor such as calcium (Sakurai & Kondo, 1978). Dancer et al. (1990) proposed a calcium binding site based upon sequence identity with a known calcium binding motif. A careful examination of the electron density maps of both crystal forms II and IV revealed no $F_o - F_c$ feature or geometry consistent with a metal ion binding site.

The structural models of ETA in crystal forms II and IV are very similar. The root-mean-square (RMS) deviation for the Cα trace is 0.44 Å while that for all atoms is 0.90 Å. The largest deviations in side chain conformations occur on the surface generally near those residues involved in differing intermolecular contacts. Consequently, further discussion of the structure of ETA will refer to that of crystal form IV unless otherwise noted.

ETA Is a Serine Protease. The overall structure of ETA is similar to the chymotrypsin-like serine protease family of enzymes (see Figure 2). Like other members of this protease family ETA has two perpendicular β-barrel domains with a carboxyl-terminal helix (αC). Structurally ETA appears to be more closely related to the mammalian serine proteases than to the relatively smaller microbial serine proteases. Superimposition of the Cα trace of ETA with those of the mammalian serine proteases finds 148−165 homologous pairs producing RMS deviations ranging from 1.49 Å for α-thrombin (Bode et al., 1989) (see Figure 3) to 2.05 Å for collagenase. Superimposition of the Cα trace of ETA with those of the microbial serine proteases finds 118−138 homologous pairs producing RMS deviations ranging from 1.71 Å for *Achromobacter* protease to 2.07 Å for glutamic acid specific *Streptomyces griseus* protease (Glu-SGP) (Nienaber et al., 1993). From the structural homology the amino acid sequence of ETA can be aligned with those of other serine proteases (see Figure 4). The positions of the three residues involved in the catalytic triad—His72(57), Asp120(102), and Ser195(195), predicted in earlier reports (Bailey & Smith, 1990; Dancer et al., 1990)—superimpose with those of α-thrombin with an RMS deviation for all atoms of 0.45 Å.

ETA Has a Unique Amino-Terminal Domain. Unlike the other members of the chymotrypsin-like family ETA has an amino-terminal domain which includes an amphipathic 15-residue α helix (αN), an extended segment containing a helical loop, a 3-residue β strand (βN) which makes three hydrogen bonds with residues His170(155)−Ser172(157) of the carboxyl-terminal β barrel (see Figure 2), and a 4-residue helix αNa. This domain is somewhat similar to the separate A-chain of thrombin in terms of secondary structure elements, but they differ in their relative positions (see Figure 3). Helix αN of ETA is highly charged with four lysine and four glutamic acid residues in the four-turn α helix. As can be seen in Figure 4, the amino acid sequence of ETB has a similarly charged amino terminus with most of these residues conserved. That the amino-terminal domain of the ETs is unique suggests this region is likely an important feature of the toxins and may participate in binding a specific receptor.

Helix αN extends across the bottom of the carboxyl-terminal β-barrel adjacent to the S1[3] binding site of chymotrypsin-like proteases contacting residues of loop 1[4] [residues 187(184)−189(189)] (see Figure 2). With the location of helix αN, loop 1 is shorter than that of thrombin and is similar in length to that of the microbial protease Glu-SGP (Nienaber et al., 1993). The helix αN also contacts loop 2 [residues 213(216)−221(223)] and prevents this loop from folding into the conformation seen in other serine proteases (see Figures 2 and 3). Loop 2 is thought to be important for the proper positioning of substrate in the active site of serine proteases as residues along the loop form hydrogen bonds with substrate (Perona & Craik, 1995). Leu217(220), whose main chain conformation is in a disallowed region of the Ramachandran plot ($\phi = 72.0°$, $\psi = -56.7°$), is located near the tip of loop 2. In ETA this loop forms an open groove on the surface of the protein as in the microbial proteases SGP-A, SGP-B, and Glu-SGP instead of a pocket as in the mammalian proteases, e.g., thrombin. However, in ETA the surface groove is much wider than those in the microbial enzymes because of the position of the αN helix.

ETA Cleaves on the Carboxyl-Terminal Side of Glutamic Acid. A superposition of the Cα trace of Glu-SGP containing

[3] Substrate residues are represented by P*n*, ..., P2, P1, P1′, P2′, ..., P*n*′, where the bond is cleaved between P1−P1′, while S*n*, ..., S2, S1, S1′, S2′, ..., S*n*′ represents the corresponding binding sites on the protein following the convention of Schechter and Berger (1968).

[4] Loops are named as described in Perona and Craik (1995).

FIGURE 3: Superimposition of Cα traces of ETA (solid lines) with both the A (dashed lines with marker Cα's) and B (dashed lines) chains of thrombin.

```
           1A              1L         10          20     26      27                   38
THROM  : cglrplfekksledkterelleyidgrIVEGSDAEIGM-----SPWQVMLFRKSPQELLCGASLISD--
           1                    20                     40                   60
ETA    :  EVSAEEIKKHEEKWNKYYGVNAFNLPKELFSKVDEKDRQKYPYNTIGNVFVK--GQTSATGVLIGK--
ETB    : KEYSAEEIRKLKQKFEVPPTD------KELYTHITDNARS--PYNSVGTVFVK--GSTLATGVLIGK--
             <----- αN ----->           β N  <αNa>        < βA1 >    < βB1 >
V8     :                         VILPNNDRHQITDTTNGHYAPVTYIQVEAPT-GTFIASGVVVGK--
GLUSGP :                                              VLGGGAIYG---GGSRCSAAFNVTKG

          50           62A       63      70      75A   80A                92A     100
THROM  : --RWVLTAAHCLLYPPWDKNFTENDLLVRIGKHSR--TRYERNIEKISMLEKIYIHPRYNWRENLDRDI
                                 80                   100                         120
ETA    : --NTVLTNRHIAKFANG----DPSKVSFRPSINTD-DNGNTETPYGEYEVKEILQEPFGA-----GVDL
ETB    : --NTIVTNYHVAREAAK----NPSNIIFTPAQNRDAEKNEFPTPYGKFEAEEIKESPYGQ-----GLDL
           β C1 <-|αA ->        β D1a D1b      E1a     β E1b
V8     : --DTLLTNKHVVDATHG---DPHALKAFPSAINQD------NYPNGGFTAEQITKY-------SGEGDL
GLUSGP : GARYFVTAGHCTNIS----------ANWSASSGGS------------VVGVREGTS-------FPTNDY
                  *                                                           *

              110    111   118     126    128               145        151
THROM  : ALMKLKK---PVAFSDYIHPVCLPDRETAASLLQAGYKGRVTGWGNLKETWTANVGKGQPSVLQVVNLP
                             140                     160
ETA    : ALIRLKPDQNGVSLGDKISPAKIGTS----NDLKDGDKLELIGYPFDH----------KVNQMHRSEIE
ETB    : AIIKLKPNEKGESAGDLIQPANIPDH----IDIQKGDKYSLLGYPYNY----------SAYSLYQSQIE
         <βF1>                                <-βA2->                 <--βB2-
V8     : AIVKFSPNEQNKHIGEVVKPATMSNN----AETQVNQNITVTGYPGDK----------PVATMWESKGK
GLUSGP : GIVRYTDGSSPAGTVDLYNGSTQDISSAAN--AVVGQAIKKSGSTT-----------------KVTSGT

            166            180            188          202    206
THROM  : IVERPVCKDSTRIRITDNMFCAGYKPDEGKRGDACEGDSGGPFVMKSPFNNRWYQMGIVSWGEGCDRDG
            180                                          200
ETA    : LTTLS-------------RGLRYY--------GFTVPGNSGSGIFNS-----NGELVGIHSSKVSHLDRE
ETB    : MFND----------------SQYF--------GYTEVGNSGSGIFNL-----KGELIGIHSGKGGQHNLP
         ->                  β C2                βD2          <-- βE2-->
V8     : ITYL--------------KGEAMQY------DLSTTGGNSGSPVFNE-----KNEVIGIHWGGVPNEFNG
GLUSGP : VTAVNVTVNY-GDGPVYNMVRTT--------ACSAGGDSGGAHFAG------SVALGIHSGSS-GCSGT
                                          #     *                  #   #

          224        233        243
THROM  : -KYGFYTHVF-RLKKWIQKVIDQ
          221                240
ETA    : HQINYGVGIGNYVKRIINEKNE
ETB    : IGVFFNRKISSLYSVDNTFGDTLGNDLKKRAKLDK
          <-βF2->  <---αC--->
V8     : AVINENVRNFLKQNIEDIHFANDDQPNNPDNPDNPNNPDNPNNPDEPNNPDNPNNPDNPDNGD
GLUSGP : AGSAIHQPV-TEALSAYGVTVYAAPE
```

FIGURE 4: Amino acid alignment of thrombin (including the A-chain in lower case), ETA, ETB, staphylococcal V8 protease, and Glu-SGP. Sequential numbering of ETA residues is above its amino acid sequence; chymotrypsin numbering is above the sequence of thrombin. Secondary structural elements of ETA are indicated under the sequence of ETB. Residues of the catalytic triad (*) and those that bind acidic residues at the S1 site (#) are indicated.

its bound inhibitor (Nienaber et al., 1993) with that of ETA indicates that the S1 binding site of ETA is complementary to a glutamic acid residue (Glu P1; see Figure 5a). The conservation of the histidine directly interacting with Glu P1 in Glu-SGP and of a threonine/serine side chain hydroxyl presumably critical for the positioning of substrate, i.e., His210(213) and Thr190(190) in ETA, led Nienaber et al. (1993) to suggest a similar motif for proteases that cleave after acidic residues. In Glu-SGP a novel triplet of histidine residues is responsible for neutralizing the negative charge of Glu P1. However, there is no comparable triad of histidine residues in ETA.

Prior to the determination of the structure of Glu-GSP it was predicted that a lysine or arginine would be involved in the charge stabilization of an acidic residue in the S1 binding site (Graf et al., 1987; Koniyama et al., 1991). Although this prediction was incorrect for Glu-SGP, it does seem to be the case for ETA where Lys213(216) Nζ is 2.8 Å from a carboxyl O of the glutamic acid modeled in the S1 binding site (Figure 5a). This lysine is conserved in ETB, but the

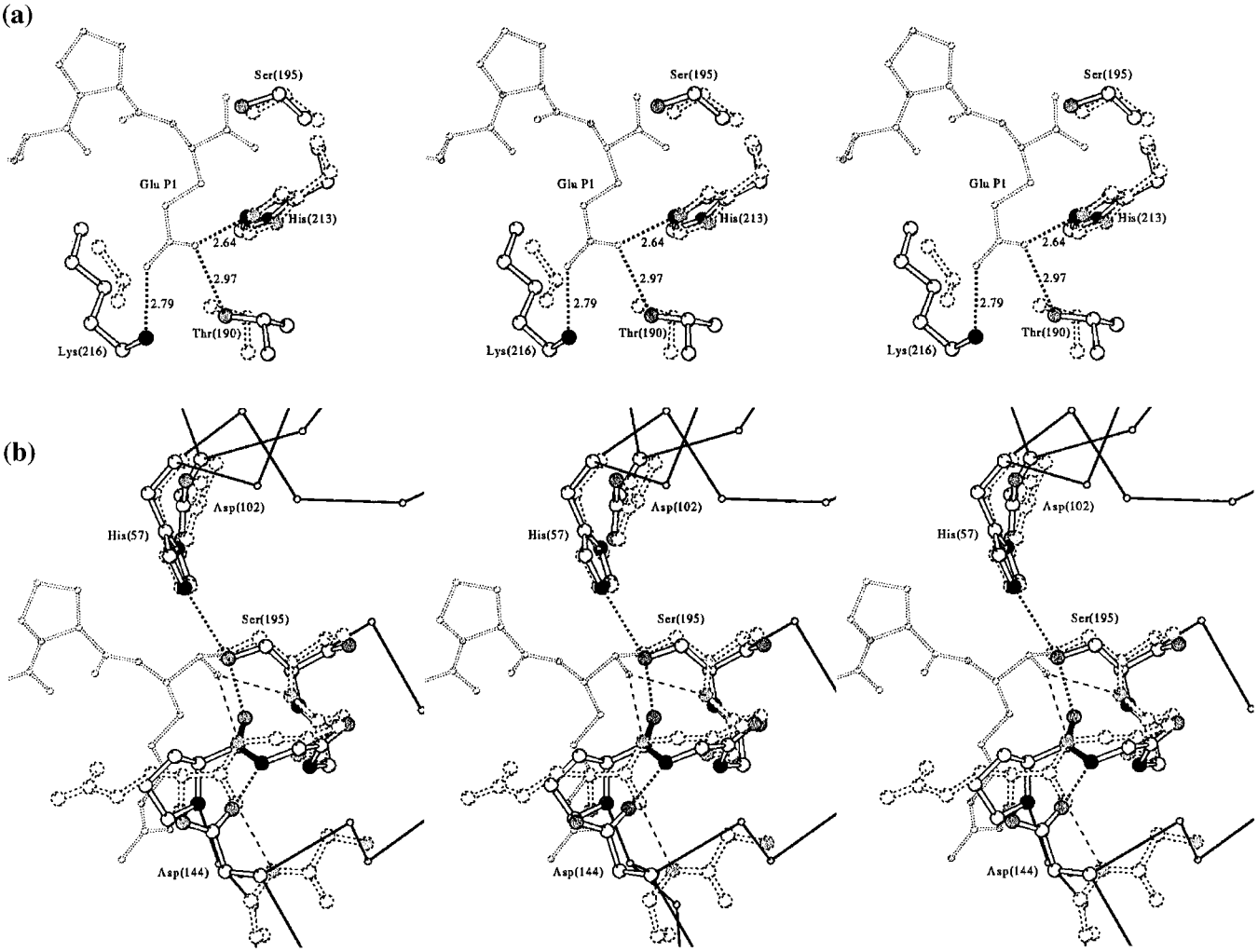

FIGURE 5: (a) Stereo drawing of the S1 binding site of Glu-SGP (dashed thick bonds) with bound inhibitor (dashed thin bonds) superimposed on that of ETA (solid thick bonds). Carbon atoms are in white; nitrogen atoms are in dark gray; oxygen atoms are in light gray. Distances from ETA atoms Thr190(190) Oγ, His210(213) Nϵ2, and Lys213(216) Nζ to the modeled Glu P1 are shown. (b) Stereo drawing of the active site of thrombin (dashed thick bonds) with bound inhibitor (dashed thin bonds) superimposed upon that of ETA (solid thick bonds). Hydrogen bonds for thrombin (thin dashed lines) and ETA (thick dashed lines) are included. Cα traces (thick solid lines) are that of ETA. The flipped peptide bond in ETA is shown with black bonds.

homologous residue in staphylococcal V8 protease is a glycine leaving its counterion for Glu P1 open to speculation.

Biological Activity of ETA and the S195C Mutant. The unique property of ETA is the ability to cause the specific separation of epidermal layers. Previously, it was reported that the S195C mutant of ETA is incapable of causing the positive Nikolsky sign (Prevost et al., 1990). This observation was confirmed in the present study. All three mice receiving wild-type ETA showed skin separation while none of the three mice receiving the S195C mutant showed a positive response after 3 h. Injection of mice with subtilisin showed a general necrosis at the site of injection while injection with trypsin caused inflammation but no skin separation. These results suggest that skin separation is the result of a very specific proteolysis by ETA.

The second property of ETA is its mitogenicity. Studies shown in Figure 6 reflect two important results. First these studies verify that ETA is mitogenic. The previous suggestion that the reported mitogenicity of ETA was due to contamination by another superantigen (Fleischer & Bailey, 1992) is unlikely as the recombinant wild-type and mutant ETA were purified from a superantigen-free strain of *S. aureus*. The second observation is that the S195C mutant of ETA is essentially as mitogenic as wild-type protein. Thus mitogenic and proteolytic activities are distinct and separable properties of the ETs. This multifunctionality of staphylococcal or streptococcal toxins is not new. TSST-1 despite strong structural homology with the staphylococcal enterotoxins is not emetic even though it has full mitogenic activity [for a review see Bohach et al. (1990)]. More recently, Murray et al. (1995) have demonstrated that lethality and mitogenicity are separable properties in TSST-1. The significant drop in mitogenicity at high concentrations of the S195C mutant as seen in Figure 6 is interesting and warrants further study.

Proteolytic Activity of ETA. The structure of ETA and the inability of the S195C mutant to produce the positive Nikolsky sign imply that ETA has proteolytic activity in vivo. Accepting this, the question is why do the ETs not display any proteolytic activity in vitro? The answer appears to reside in the observation that the peptide bond between Pro192(192) and Gly193(193) is flipped 180° relative to that typically seen in other serine proteases (see Figures 1 and 5b). The main chain nitrogen of the conserved Gly193(193), which has been shown to be important for stabilization of the tetrahedral intermediate, forms a hydrogen bond with the

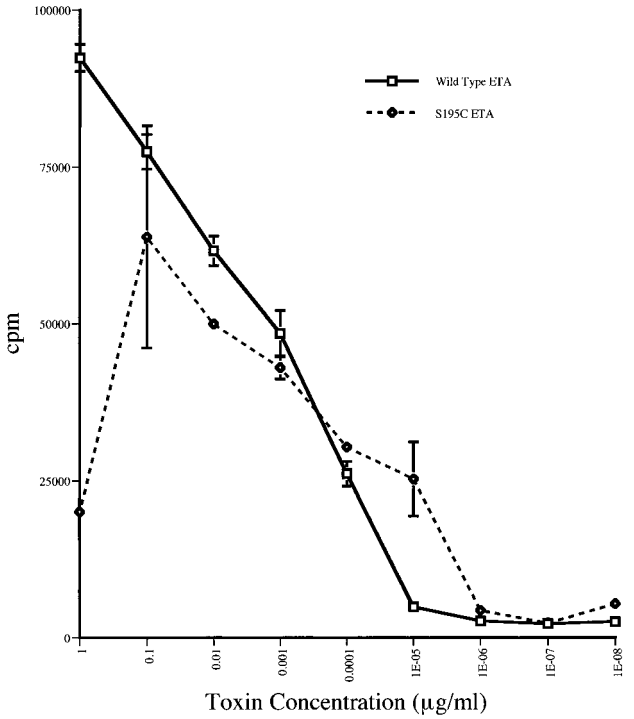

FIGURE 6: Mitogenicity of wild-type and S195C ETA measured by incorporation of [^{3}H]thymine in human lymphocytes. Each measurement was done in quadruplicate, and all error bars are indicated (in some cases the error bars are hidden behind the symbol).

side chain carboxyl of Asp164(144) in loop D [residues 163-(143)−168(153)]. This arrangement places the carbonyl oxygen of Pro192(192) within 3.1 Å of the reactive Ser195-(195), blocking substrates and inhibitors from binding in the oxyanion hole and forming the proper tetrahedral intermediate. In thrombin the carbonyl oxygen of Glu192 forms a hydrogen bond with the main chain N of Asn143 of loop D while the analogous hydrogen bond found in Glu-SGP is with the side chain of Thr142.

The backbone conformation of the segment of ETA containing the Pro−Gly bond is not unique to ETA. Pro192(192) has a helical conformation with $\phi = -46.4°$ and $\psi = -40.8°$ while Gly193(193) also has a helical conformation with $\phi = -59.1°$ and $\psi = -21.3°$. There are three examples in the most recent release of the Protein Data Bank of hexapeptides with backbone atoms differing from those seen in residues 190(190)−195(195) of ETA by less than 0.4 Å (RMS). In addition, Allaire et al. (1994) reported a similar orientation of the Pro−Gly peptide bond in a mutant of hepatitis A virus 3C protease in which the active site cysteine had been changed to an alanine. The authors concluded, however, that this conformation is not biologically relevant as the sulfur of the cysteine in the wild-type enzyme would likely prevent the flipping of the carbonyl oxygen of the Pro. This hypothesis has been confirmed in the structure of the wild-type hepatitis 3C protease (Bergmann et al., 1997).

Given the results of this structural analysis and the highly specific nature of skin separation, the activation of the proteolytic activity of ETA appears to be regulated through binding another molecule such as a specific receptor. This binding may involve the αN helix and produce a shift in loop D allowing the peptide bond between Pro192(192) and Gly193(193) to flip to the consensus conformation and form a hydrogen bond between the carbonyl O of Pro192(192) and the amide N of Asp164(144) leading to protease activation. There are several example of other proteases whose activities are controlled by other molecules. These include thrombin [see Gerskkovich (1996) for a recent review] and hepatitis C virus NS3 protease where the NS4A cofactor peptide is inserted into the N-terminal β-barrel of the protease (Kim et al., 1996).

The novel conformation of Pro192(192) and Gly193(193) in ETA suggests that the side chain of His72(57) of the catalytic triad may be protonated. In the conformation seen in ETA, the hydrogen on the side chain hydroxyl of Ser195(195) is participating in a hydrogen bond with the carbonyl oxygen of Pro192(192) (d(O···N) = 3.1 Å). However the distance between His72(57) Nϵ2 and Ser195(195) Oγ of only 3.0 Å suggests a hydrogen bond between these residues requiring a proton on the nitrogen atom.

Mitogenic Activity of ETA. Currently the mechanism by which ETA acts as a mitogen is unknown. The pyrogenic toxin superantigens stimulate T cells by forming a bridge between the α chain of a class II major histocompatibility complex molecule (Jardetsky et al., 1994; Kim et al., 1994) and the variable region of the β chain of the T cell receptor (Fields et al., 1996). As there is no structural homology between ETA and any of the pyrogenic superantigens, the structural basis for its mitogenicity is uncertain. Studies by Bar-Shavit et al. (1986) have suggested that thrombin is mitogenic for macrophage-like cells independent of its protease activity. The region of thrombin believed responsible for its protease-independent mitogenic activity has been proposed to be an insertion loop not seen in other serine proteases involving residues Tyr60A-Pro60H (chymotrypsin numbering) (see Figure 4). This loop is also absent in ETA.

The role of mitogenicity in staphylococcal scalded skin syndrome is also poorly understood. Mitogenicity (or superantigenicity) may be involved in the edema or redness associated with the syndrome. The proliferation of T cells in scalded skin syndrome is limited or may not occur systemically when compared to that which occurs in toxic shock syndrome since it is normally nonfatal with a minimal fever.

CONCLUSION

The structure of ETA conclusively shows that the ETs are serine proteases which cleave after acidic residues as previously predicted. Catalytic activity of ETA appears to be regulated through a novel conformational flip of a main chain peptide bond. Thus the specificity of proteolysis may be modulated through a specific interaction of the unique N-terminal domain and loop D with another molecule. The mitogenic and proteolytic properties of ETA are independent.

ACKNOWLEDGMENT

The authors acknowledge the Minnesota Supercomputer Institute for the use of computational resources, the reviewers for pointing out the hepatitis virus proteinase results, and Dr. Michael James for providing data on the wild-type hepatitis virus 3C protease prior to publication.

REFERENCES

Acharya, K. R., Passalacqua, E. F., Jones, E. Y., Harlos, K., Stuart, D. I., Brehm, R. D., & Tranter, H. S. (1994) *Nature 367*, 94−97.

Allaire, M., Chernaia, M. M., Malcolm, B. A., & James, M. N. G. (1994) *Nature 369*, 72−76.
Bailey, C. J., & Smith, T. P. (1990) *FEBS Lett. 269*, 535−537.
Bailey, C. J., Lockhart, B. P., Redpath, M. B., & Smith, T. P. (1995) *Med. Microbiol. Immunol. 184*, 53−61.
Bar-Shavit, R., Kahn, A. J., Mann, K. G., & Wilner, G. D. (1986) *Proc. Natl. Acad. Sci. U.S.A. 83*, 976−980.
Barsumian, E. L., Schlievert, P. M., & Watson, D. W. (1978) *Infect. Immun. 22*, 681−688.
Bergmann, E. M., Mosimann, S. C., Chernaia, M. M., Malcom, B. A., & James, M. N. G. (1997) *J. Virol.* (in press).
Bode, W., Mayr, I., Baumann, U., Huber, R., Stone, S. R., & Hofsteenge, J. (1989) *EMBO J. 8*, 3467−3475.
Bohach, G. A., Fast, D. J., Nelson, R. D., & Schlievert, P. M. (1990) *Crit. Rev. Microbiol. 17*, 251−272.
Brünger, A. T. (1990) *X-PLOR Version 3: A System for Crystallography and NMR*, Yale University Press, New Haven, CT.
Collaborative Computational Project, Number 4 (1994) *Acta Crystallogr. D50*, 760−763.
Cowtan, K. (1994) *Joint CCP4 and ESF-EACBM Newsletter on Protein Crystallography*, Vol. 31, pp 34−38.
Dancer, S. J., Garratt, R., Saldanha, J., Jhoti, H., & Evans, R. (1990) *FEBS Lett. 268*, 129−132.
Elias, P. M., Fritsch, P., & Epstein, E. H. (1977) *Arch. Dermatol. 113*, 207−219.
Fields, B. A., Malchiodi, E. L., Li, H., Ysern, X., Stauffacher, C. V., Schlievert, P. M., Karjalainen, S., & Mariuzza, R. A. (1996) *Nature 384*, 188−192.
Fleischer, B., & Bailey, C. J. (1992) *Med. Microbiol. Immunol. 180*, 273−278.
Gershkovich, A. A. (1996) *Biochemistry (Moscow) 61*, 817−824.
Graf, L., Craik, C. S., Patthy, A., Roczniak, S., Fletterick, R. J., & Rutter, W. J. (1987) *Biochemistry 26*, 2616−2623.
Hoffmann, M. L., Jablanski, L. M., Crum, K. K., Hackett, S. P., Chi, Y. I., Stauffacher, C. V., Stevens, D. L., & Bohach, G. A. (1994) *Infect. Immun. 62*, 3396−3407.
Howard, A. J., Gilliland, G. L., Finzel, B. C., Poulos, T. L., Ohlendorf, D. H., & Salemme, F. R. (1987) *J Appl. Crystallogr. 20*, 383−387.
Jardetsky, T. S., Brown, J. H., Gorga, J. C., Stern, L. J., Urban, R. G., Chi, Y.-I., Stauffacher, C. V., Strominger, J. L., & Wiley, D. C. (1994) *Nature* 368, 711−718.
Jones, A. T., Zou, J. Y., Cowan, S. W., & Kjeldgaard, M. (1991) *Acta Crystallogr. A47*, 110−119.
Kim, J., Urban, R. G., Strominger, J. L., & Wiley, D. C. (1994) *Science 266*, 1870−1874.
Kim, J. L., Morgenstern, K. A., Lin, C., Fox, T., Dwyer, M. D., Landro, J. A., Chambers, S. P., Markland, W., Lepre, C. A., O'Malley, E. T., Harbeson, S. L., Rice, C. M., Murcko, M. A., Caron, P. R., & Thomson, J. A. (1996) *Cell 87*, 343−355.
Komiyama, T., Bigler, T. L., Yoshida, N., Noda, D., & Laskowski, M. (1991) *J. Biol. Chem. 266*, 10727−10730.
Laskowski, R. A., MacArthur, M. W., Moss, D. S., & Thornton, J. M. (1993) *J. Appl. Crystallogr. 26*, 283−291.
Lee, C. Y., Schmidt, J. J., Johnson-Winegar, A. D., Spero, L., & Iandolo, J. J. (1987) *J. Bacteriol. 169*, 3904−3909.
Lee, P. K., Deringer, J. R., Kreiswirth, B. N., Novick, R. P., & Schlievert, P. M. (1991) *Infect. Immun. 59*, 879−884.
Levitt, G., & Banaszak, L. J. (1993) *J. Appl. Crystallogr. 26*, 736−745.
Marrack, P., & Kappler, J. (1990) *Science 248*, 705−711.
McLay, A. L. C., Arbuthnott, J. P., & Lyell, A. (1975) *J. Invest. Dermatol. 65*, 423−428.
Melish, M. F., Glasgow, L. A., & Turner, M. D. (1972) *J. Infect. Dis. 125*, 129−140.
Morlock, B. A., Spero, L., & Johnson, A. D. (1980) *Infect. Immun. 30*, 381−384.
Murray, D. L., Earhart, C. A., Mitchell, D. T., Ohlendorf, D. H., Novick, R. P., & Schlievert, P. M. (1995) *Infect. Immun.* 64, 371−374.
Navaza, J. (1994) *Acta Crystallogr. A50*, 157−163.
Nienaber, V. L., Breddam, K., & Birktoft, J. J. (1993) *Biochemistry 32*, 11469−11475.
Nishioka, K., Katayama, I., & Sano, S. (1981) *J. Dermatol. 8*, 7−12.
O'Toole, P. W., & Foster, T. J. (1987) *J. Bacteriol. 169*, 3910−3915.
Papageorgiou, A. C., Acharya, K. R., Shapiro, R., Passalacqua, E. F., Brehm, R. D., & Tranter, H. S. (1995) *Structure 3*, 769−779.
Perona, J. J., & Craik, C. S. (1995) *Protein Sci. 4*, 337−360.
Prasad, G. S., Earhart, C. A., Murray, D. L., Novick, R. P., Schlievert, P. M., & Ohlendorf, D. H. (1993) *Biochemistry 32*, 13761−13766.
Prevost, G., Rifai, S., Chaix, M. L., & Piemont, Y. (1991) *Infect. Immun. 59*, 3337−3339.
Prevost, G., Rifai, S., Chaix, M. L., Meyer S., & Piemont, Y. (1992) in *Bacterial protein toxins* (Witholt, B., et al., Eds.) pp 488−489, Fischer, Stuttgart.
Redpath M. B., Foster T. J., & Bailey C. J. (1991) *FEMS Microbiol. Lett. 81*, 151−156.
Rogolsky, M. (1979) *Microbiol. Rev. 43*, 320−360.
Sakurai, S., & Kondo, I. (1978) *Jpn. J. Med. Sci. Biol. 31*, 208−211.
Schad, E. M., Zaitseva, I., Zaitsev, V. N., Dohlsten, M., Kalland, T., Schlievert, P. M., Ohlendorf, D. H., & Svensson, L. A. (1995) *EMBO J. 14*, 3292−3301.
Schechter, I., & Berger, A. (1968) *Biochem. Biophys, Res. Commun. 27*, 157−162.
Swaminathan, S., Furey, W., Pletcher, J., & Sax, M. (1992) *Nature 359*, 801−806.
Wuepper, K. D., Dimond, R. L., & Knutson, D. D. (1975) *J. Invest. Dermatol. 65*, 191−200.
Yoo, C. S., Wang, B. C., Sax, M., & Johnson, A. D. (1978) *J. Mol. Biol. 175*, 421−423.

BI962614F